Ankara Üniversitesi Veteriner Fakültesi Dergisi/Ankara Univ Vet Fak Derg; 2026:73(4): 364-379
DOI: 10.33988/auvfd.1842868
Research Article

Cytokine profiles and genetic variations based on mitochondrial ND1 and COX1 genes of *Coenurus cerebralis* in Türkiye

Gökben ÖZBAKIŞ BECERİKLİSOY[1,a,✉], Emin KARAKURT[2,b,✉], Bengi ÇINAR[3,c], Serpil DAĞ[2,d], Enver BEYTUT[2,e], Hilmi NUHOĞLU[2,f], Ayfer YILDIZ UYSAL[2,g]

[1]Ankara University, Faculty of Veterinary Medicine, Department of Parasitology, Ankara, Türkiye;
[2]Kafkas University, Faculty of Veterinary Medicine, Department of Pathology, Kars, Türkiye;
[3]Ankara University, Faculty of Veterinary Medicine, Department of Genetics, Ankara, Türkiye.

[a]ORCID: 0000-0002-3354-9150; [b]ORCID: 0000-0003-2019-3690; [c]ORCID: 0000-0002-8955-0097; [d]ORCID: 0000-0001-7667-689X; [e]ORCID: 0000-0003-3360-2940; [f]ORCID: 0000-0003-2530-2542; [g]ORCID: 0000-0002-6569-5435.

ABSTRACT

Coenurosis, caused by the metacestode (*Coenurus cerebralis*) of *Taenia multiceps*, is a significant zoonotic parasitic disease that primarily affects the small ruminants, resulting in economic difficulties within the livestock industry. This study first aimed to evaluate the expression of cytokines, including Interleukin (IL)-1β, 2, 6, 8, 10, 12, Tumor Necrosis Factor Alpha (TNF-α) and Interferon Gamma (IFN-γ) via immunohistochemical methods and the second objective was to performed molecular analyses including phylogenetic and haplotype assessments of the mitochondrial cytochrome c oxidase subunit 1 (COX1) and NADH dehydrogenase subunit 1 (ND1) genes of *C. cerebralis* isolates obtained from sheep in Türkiye. Ten sheep brains infected with *C. cerebralis* were examined. Foreign body granulomatous reactions were detected in six animals. All animals were recorded positive for immunohistochemically for TNF-α, IFN-γ, and Interleukins. Molecular analysis of the COX1 and ND1 genes positive results were obtained in twelve cysts from ten animals. The isolates revealed four different haplotypes out of 30 haplotypes for the COX1 gene and 9 distinct haplotypes (six unique) out of 46 for the ND1 gene. Among the two animals with multiple *C. cerebralis* cysts, ND1 sequencing revealed four distinct haplotypes, whereas COX1 sequencing showed that one of these animals harboured two distinct haplotypes. When potential relationships between the IHC results and the haplotype distributions of the cases were examined, no consistent association emerged between particular lineages and granuloma formation, clinical findings or cytokine expression profiles. These findings enhance the understanding of cytokine expression patterns and genetic diversity of *C. cerebralis* in Türkiye.

Keywords: Coenurosis, Haplotype diversity, Immunohistochemistry, Phylogenetic analysis, *Taeina multiceps*

✉**Corresponding authors:** ozbakis@ankara.edu.tr; eminkarakurt@kafkas.edu.tr
Received: 15.12.2025, **Accepted:** 16.02.2026, **Publication Date:** 01.10.2026

How to cite this article: Özbakış Beceriklisoy G, Karakurt E, Çınar B, Dağ S, Beytut E, Nuhoğlu H, Yıldız Uysal A (2026): Cytokine profiles and genetic variations based on mitochondrial ND1 and COX1 genes of *Coenurus cerebralis* in Türkiye. Ankara Univ Vet Fak Derg, 73 (4), 364-379. DOI: 10.33988/auvfd.1842868.

Introduction

Coenurus cerebralis (*C. cerebralis*), larva of *Taenia multiceps* (Leske 1780), is the cause of coenurosis, also known as sturdy, gid or staggers, a neuropathological disease that affects sheep, goats, cattle, pigs, horses, deer, camels, and humans (42, 44, 45, 60). Among the wide variety of domestic and wild animals acting as intermediate hosts, sheep and goats are particularly notable (2).

Taenia multiceps (T. multiceps) has a complex life cycle that involves two hosts (2, 60). The infection circulates in the environment via the feces of definitive hosts (dogs, foxes and wild canids), which contain *T. multiceps* eggs or gravid proglottids (44, 60). An intermediate host ingests eggs, the oncosphere penetrates the intestinal wall and primarily affects the central nervous system (CNS) via the bloodstream, where it encysts. The metacestode can also be located in extra-CNS such as

subcutaneous and intramuscular tissues, peritoneal areas, and internal organs (the heart and lungs) of sheep and goats (60).

Coenurosis exhibits a global distribution and has been reported in Europe, Asia and Africa (60). *C. cerebralis* has been also recorded in various intermediate hosts, including sheep (3, 11, 15, 17, 29, 31), mountain goats (31), wild goat (56) and cattle (10, 31) in Türkiye. The infection causes significant economic losses in small ruminants (2, 6, 60). The zoonotic importance of the parasite has been confirmed via several cases of coenurosis in humans caused by *T. multiceps* (18, 60).

Inflammatory mediators of the host play a critical role in the immunopathogenesis of various parasitic diseases (46, 61). Cytokines mediate the intercellular communication among immune, endocrine and nervous systems. Cytokines can be classified in different categories according to their functions including tumor necrosis factors, interleukins, interferons, and colony-stimulating factors (38). In response to various pathogens, including parasitic ones, naive CD4+ T cells differentiate to effector Th1 and/or Th2 cells. Th1 cells produce IL-2, IFN-γ, and TNF-α, and take part in cell-mediated immune responses. Th2 cells primarily secrete IL-4, IL-5, IL-6, IL-10, and IL-13, regulating B cell activation, antibody production, and Th1 responses. In many instances, Th1-type immune responses aid in the elimination of intracellular microorganisms, while Th2-type immune responses are more effective in controlling extracellular pathogens (55). Most helminths have developed complex mechanisms to evade and regulate the host's immune system. It has been demonstrated that macrophages play a central role in the immune response to helminth infections (48). Macrophages can be classified in two categories: classically activated (M1) and alternatively activated (M2) macrophages. M1 macrophages, activated by lipopolysaccharide (LPS) and IFN-γ, produce IL-6, IL-12, and TNF-α, and are highly effective in the immune response against intracellular parasites (43). Mixed Th1/Th2 cytokine production has been observed in response to helminth infections. In this immune response, especially during the early stages of infection, Th1 inflammatory responses dominate, whereas the response shifts towards Th2 as the disease progresses (36, 48).

The sequencing of mitochondrial DNA genes, including COX1 and ND1, is utilized successfully for the molecular characterization and phylogenetic analysis of *Taenia* species. The control of taeniid cestodes depends on epidemiological data, which include a precise detection and characterization of the causal agent (23). Comprehending the genetic diversity of *T. multiceps* could clarify its transmission patterns and potential management strategies (14, 15, 37).

It is firstly aimed to evaluate the expression of cytokines, including Interleukin (IL)-1β, 2, 6, 8, 10, 12, Tumor Necrosis Factor Alpha (TNF-α) and Interferon Gamma (IFN-γ) via immunohistochemical methods to assess the immune response in sheep with *C. cerebralis* in more detail. The second objective was to perform molecular analyses including phylogenetic and haplotype analysis of two mitochondrial COX1 and ND1 genes of *C. cerebralis* in sheep in Türkiye.

Materials and Methods

Samples Collection: The brain tissues obtained from 10 sheep, between 5-12 months of age, which were submitted to the Kafkas University Faculty of Veterinary Medicine, Department of Pathology for routine histopathological analyses between 2020 and 2021 (Table 1). According to the anamnesis provided by the animal owners, several clinical symptoms were recorded in the sheep, including ataxia, inability to rise, circling behavior, unilateral blindness, torticollis, and opisthotonus. Cases were clinically categorized based on the number of findings reported: mild (+) for a single finding, moderate (++) for two findings, and severe (+++) for more than two findings.

Histopathological Analysis: Brain tissue samples were fixed in a 10% buffered formalin solution. Following routine tissue fixation procedures, 5μm thick serial sections were taken from the prepared paraffin blocks. The sections were stained with Hematoxylin and Eosin (HE).

Immunohistochemical Analysis: Serial sections of the paraffin-embedded blocks were taken at 4 μm. For antigen retrieval, all sections were pretreated in a microwave oven for 25 minutes using citrate buffer (pH 6.0). Sections were then incubated overnight at 4°C with commercial primary antibodies against TNF-α, IFN-γ, IL-1β, IL-2, IL-6, IL-8, IL-10, and IL-12, followed by the Avidin-Biotin-Peroxidase Complex (ABC) technique according to the kit procedure (Thermo Scientific Histostain IHC Kit, HRP, broadspectrum, REF: TP-125-HL). The primary antibodies, dilutions and sources are listed in Table 2.

Amino ethyl carbazole (AEC, Thermo Scientific, REF: TA-125-HA) was applied as a chromogenic substrate and incubated for 15 minutes. Sections were rinsed with distilled water for 5 minutes, stained with Mayer's Hematoxylin and covered with AEC mount. All sections were examined under a light microscope (Olympus BX53) by two different pathologists, and were photographed with the Cell^P software (Olympus Soft Imaging Solutions GmbH, 3,4). A comprehensive analysis of images was conducted with the Image J program (1.51j8).

Evaluations of immunohistochemical stainings were made using a grading system based on the number of

positive cells in the areas where immune-positive reactions were seen most prominently. Three different microscopical areas of each brain tissue were assessed utilizing a 50× objective lens. The number of positive cells was recorded individually, and the average of these three areas was taken as the mean positive cell count.

Grading was performed according to the criteria described by Karakurt et al. (30), with scores documented as negative (–) for the absence of immunoreactivity, mild (+) for 1-10% positivity, moderate (++) for 11-59% positivity, and severe (+++) for greater than 60% positivity.

Molecular Analyses: Genomic DNA was extracted from the cysts fluid (200 µL) or cyst wall (20 mg) using the GeneJET Genomic DNA Purification Kit (K0721, Thermo Fisher Scientific, Lithuania) according to the manufacturer's instructions. The template DNAs were eluted with 100 µL of elution buffer in the final step and stored at −20°C until used. The extracted DNAs were measured by a spectrophotometer (NanoDrop 2000, Thermo Scientific, USA). The mt-DNA ND1 and COX1 regions were amplified using the primers JB11 (5′-AGATTCGTAAGGGGCCTAATA-3′) - JB12 (5′-ACCACTAACTAATTCACTTTC-3′) (13) and JB3 (5′-TTTTTTGGGCATCCTGAGGTTTAT-3′) - JB4.5 (5′-TAAAGAAAGAACATAATGAAAATG-3′) (12), respectively. Each PCR reaction was carried out in a 30 µL total volume mix containing 2.0 mM $MgCl_2$, 0.5 µM of each primer, 0.2 µM dNTPs, 1 IU Dream Taq DNA Polymerase (Thermo Scientific, Lithuania), 10× Dream Taq buffer and approximately 50 ng of template DNA. The PCR protocols were as follows: initial denaturation at 95 °C for 5 min followed by 35 cycles of denaturation at 95 °C for 45 s, annealing at 53 °C for 45 s, extension at 72 °C for 45 s, and completing with a final extension at 72 °C for 5 min. SafeView-stained 2% agarose gel electrophoresis in TBE buffer at 100 V for 30 minutes was used to confirm and visualize the amplicons using a UV transilluminator (Kodak Gel Logic 200 imaging system, Eastman Kodak Company, USA). PCR amplicons for the COX1 and ND1 genes were commercially sequenced in both directions (Invitrogen, Ankara, Türkiye). The raw data were manually checked and aligned using BioEdit (25). Following the sequence alignment 482 bp and 337 bp were obtained for ND1 and COX1, respectively. All sequences were verified with the Basic Local Alignment Search Tool (BLAST) as *T. multiceps* in both adult and larval form. All sequences were aligned with the reference sequences from whole genome sequence of *T. multiceps* (GeneID 8097138 for ND1, and GeneID 8097137 for COX1 in NC_012894). Additionally, previously published sequences for ND1 and COX1 of *T. multiceps* in GenBank were used in alignment analysis (Tables 3 and 4). The evolutionary distances were computed in Molecular Evolutionary Genetics Analysis (MEGA12.0.11) software (35, 53) using the Kimura 2-parameter method (34) and a Neighbor-Joining (NJ) tree (50). Bootstrap values obtained from 1000 replicates were shown at the nodes; only values ≥70% were indicated (19). A previously reported *Taenia saginata* sequence (accession number: NC_009938.1) was used as an outgroup for both phylogenetic trees. Haplotype diversity and neutrality were calculated in DNA Sequence Polymorphism-DnaSP v6.10.04 (49). For comparison across multiple cyst samples, amino acid substitutions and their residue positions were identified by aligning each sequence to the reference in Jalview with the translation view enabled (62). Variant coordinates are reported relative to the reference coding sequence (A of the ATG start codon set as c.1), and amino acid numbering follows the corresponding translated open reading frame.

Results

Macroscopical Findings: Following the inspection of the brains, characteristic *C. cerebralis* cysts were identified (Figure 1a-b). The anatomical positions of all the metacestodes are detailed in Table 1. Six cases had a single cyst while four animals had more than one metacestode scattered throughout the parenchyma (Table 1). Numerous white, pinpoint-sized scolices were observed within the cysts. Additionally, severe meningitis, hyperemia, atrophy and necrotic foci in the brain tissue were seen.

Histopathological Findings: Histopathological examination of brain tissues revealed foreign body granulation tissue in 6 out of 10 animals. In these animals, various numbers of protoscolices were detected (Figure 1c-d). In addition, wide areas of liquefactive necrosis were observed. There were severe inflammatory cell infiltrations consisting mostly of lymphocytes, epithelioid histiocytes and plasma cells, along with a small number of eosinophil leukocytes, surrounding both necrotic foci and the parasitic cyst walls.

A large number of multinucleated foreign body giant cells with irregular borders were observed, with multiple vesicular nuclei localized opposing the membrane of the parasitic cysts. Severe hyperemia was detected in the areas around the cysts. Perivascular mononuclear cell infiltration was a notable histopathological finding. In the four animals without granuloma formation, gliosis, degenerative changes in a few neurons, thrombosis, demyelination, nonpurulent meningoencephalitis, perivascular cell infiltration, severe hyperemia and edema in the meninges were detected.

Immunohistochemical Findings: All cases with *C. cerebralis* were recorded as positive for TNF-α, IFN-γ, IL-1β, IL-2, IL-6, IL-8, IL-10 and IL-12 expressions with different scores. The immunopositivity scores of all cases are listed in Table 5. Both pro-inflammatory and anti-inflammatory cytokine immunoreactivities were much more noticeable in cases with foreign body giant cell formation. In cases with granuloma formation, positive staining for TNF-α (Figure 2a) and IFN-γ (Figure 2b) was quite intense compared to other cytokines. Both cytokines were found primarily around the cyst walls, particularly within the cytoplasm of multinucleated foreign body giant cells. There was positive staining of these cytokines in the mononuclear cells around the vessels, degenerated and healthy neurons as well as in glial cells. IL-1β (Figure 2c), IL-2 (Figure 2d), IL-6 (Figure 3a), IL-8 (Figure 3b), and IL-12 (Figure 3d) were significantly immunopositive in glial cells and inflammatory cells localized around the vessels close to the affected areas. Anti-inflammatory cytokine IL-10 (Figure 3c) expressions were found to be severely positive, particularly in foreign body giant cells, similar to TNF-α and IFN-γ.

Molecular Findings: Twelve *C. cerebralis* cysts were molecularly analyzed from ten sheep. A total of 46 haplotypes were identified, with thirty-four variable nucleotide positions, in the ND1 sequence alignment with the reference sequences (Table 3). Our isolates exhibited nine distinct haplotypes, six of which were unique sequences, and submitted to the GenBank database under the following accession numbers: PX677447-PX677458. The remaining three haplotypes are as follows: sample A10 is identical to a sheep sample from Greece in Hap-7, while the samples A1 and A3 are identical to goat samples from China, India, and Greece in Hap-8. A NJ tree was constructed with the observed haplotypes (n=46), including our isolates. The MEGA 12 program failed because the post-alignment data for haplotypes 9, 39, and 40 were short and contained numerous gaps. As a result, the phylogenetic tree was constructed excluding these three haplotypes (n=43) allowing the remaining haplotypes to be analyzed (Figure 4).

The resulting NJ topology resolved the ingroup ND1 haplotypes into three major clades (Clades I-III). Clade I comprised the most basal ingroup lineages including one sequence from the present study, A10, which corresponded to Haplotype 7. Clade II consisted of an intermediate cluster supported by bootstrap values of 86-92%. This clade harboured several newly generated unique sequences, namely A2 (Haplotype 41); A4, A8-1 and A9 (all corresponding to Haplotype 42); A6 (Haplotype 44); and A7-2 (Haplotype 45). Clade III encompassed the most apical group of haplotypes, within which a sub-clade received strong bootstrap support (96%). The remaining sequences generated in this study were also placed within this clade: A1 and A3 were identical to Haplotype 8 and A7-1 to Haplotype 37, whereas the unique sequences A5 and A8-2 corresponded to Haplotypes 43 and 46, respectively. Overall, branch lengths within the ingroup were short, consistent with low to moderate sequence divergence among ND1 haplotypes.

A total of 30 haplotypes were identified, with thirty-two polymorphic nucleotide positions, in the COX1 sequences alignment with the reference sequences (Table 4). Four various haplotypes were detected from our isolates, and these sequences were submitted to the GenBank database under the following accession numbers PX671641-PX671652. Samples B1, B3, B4, B5, B8-1, B8-2, and B9 are grouped under the same haplotype (Hap-2) and were identical to sheep isolates from Diyarbakır, Elazığ, and Mardin in Türkiye as well as from Greece, and Iran. Sample B7-1 was identic to sheep isolates from Iran and Egypt, dog isolates from Peru in the Hap-3. Samples B2, B6, and B7-2 are located in the same haplotype (Hap-4) and were found to be identical to sheep isolates from Diyarbakır, Elazığ in Türkiye and from Iran, as well as goat isolates from Iran, United Arab Emirates, China and India. The sample B10 was identic to sheep isolates from Elazığ, Niğde in Türkiye and Kazakhstan, as well as goat isolate from Greece, found in the Hap-8. A NJ tree was constructed with the observed haplotypes (n=30) including our isolates (n=12), as shown in Figure 5.

The resulting topology resolved the ingroup COX1 haplotypes into three major clades (Clades I-III). Clade I comprised the most basal lineages and contained Haplotype 18 and a strongly supported sub-clade formed by Haplotypes 3 and 25 (bootstrap 93%), with B7-1 from the present study being identical to Haplotype 3. This clade also included closely related Haplotypes 1, 15 and 20, as well as B10 from the present study, which was identical to Haplotype 8. Clade II consisted of a small intermediate cluster formed by Haplotypes 12, 13 and 14 as a branched from Clade III supported by bootstrap values of 97%. Clade III encompassed the majority of the remaining haplotypes, within which B1, B3, B4, B5, B8-1, B8-2 and B9 all corresponded to Haplotype 2, and B2, B6 and B7-2 corresponded to Haplotype 4. Thus, none of the B-labelled isolates represented novel COX1 haplotypes; instead, all of them clustered with previously described reference sequences, indicating that the COX1 diversity observed in this material is entirely encompassed by the existing haplotype framework. Overall, branch lengths within the ingroup were short, consistent with low sequence divergence among the COX1 haplotypes.

Among the four animals with multiple *C. cerebralis* cysts, only two had more than one cyst sample submitted for molecular analysis. The ND1 sequence analyses revealed that multiple cysts from two animals (samples

A8-1/8-2 and A7-1/7-2) exhibited distinct haplotypes (Hap-42/Hap-46 and Hap-37/Hap-45, respectively). Haplotypes 42, 45, and 46 possess unique sequences, while sample A7-1 of Hap-37 was found to be identical to those from sheep in Egyptian samples (Table 3). When the four sequences were aligned to the study reference sequence, comparative analysis identified two nonsynonymous single-nucleotide substitutions. First, sample A8-2 carried a c.376A>G transition, corresponding to a p.Ser126Gly (S126G) amino-acid replacement. Second, samples A7-1, A7-2, A8-1, and A8-2 all harbored a c.584G>A transition, resulting in a p.Ser195Asn (S195N) substitution. Thus, sample A8-2 exhibited co-occurrence of both variants (c.376A>G; c.584G>A), whereas the remaining three samples contained only c.584G>A. The COX1 sequence analysis showed that a single haplotype (Hap-2) represented the cysts from one animal (samples B8-1 and B8-2). In contrast the cysts from the other animal (samples B7-1 and B7-2) displayed two distinct haplotypes (Hap-3 and Hap-4) as presented in Table 4. Although several nucleotide polymorphisms were detected across the four sequences, all changes within the analyzed COX1 fragment were synonymous relative to the reference.

When the case numbers in the immunohistochemical dataset (Table 5) were cross-referenced with the mitochondrial ND1 and COX1 haplotypes, no consistent association could be identified between individual haplotypes or clades and the presence of granulomatous inflammation, clinical severity or cytokine expression profiles. Animals carrying different ND1 haplotypes (cases 7 and 8) showed marked granulomatous, Th1-biased responses, but similar patterns were also observed in cases infected with other ND1 and COX1 haplotypes.

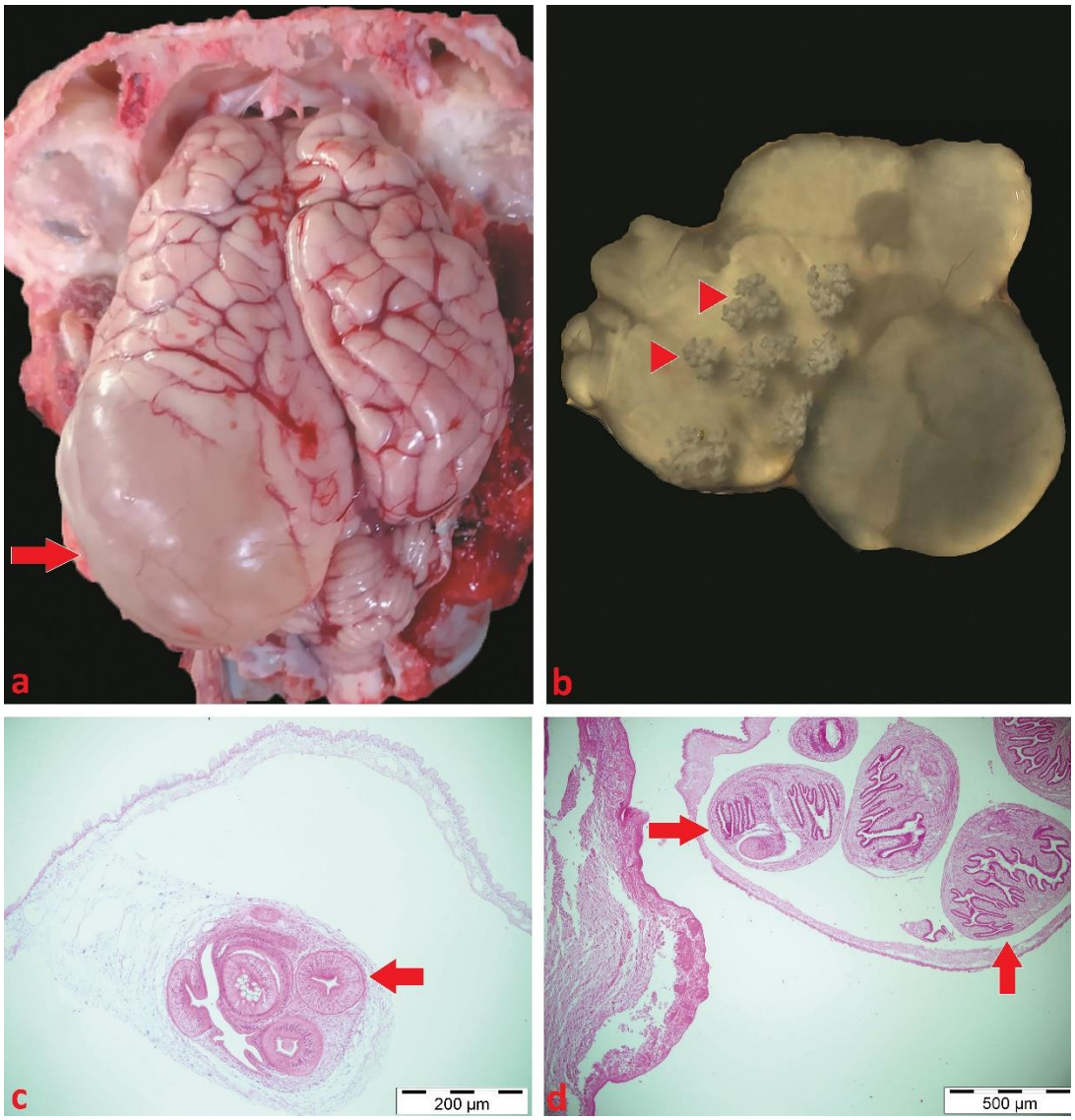


Figure 1. A view of *Coenurus cerebralis*. a: *Coenurus cerebralis* cyst (arrow) located in the left parietal lobe, b: Scolices (arrowheads), c-d: Protoscolices observed in histopathologic sections with different magnifications (arrows), HE.

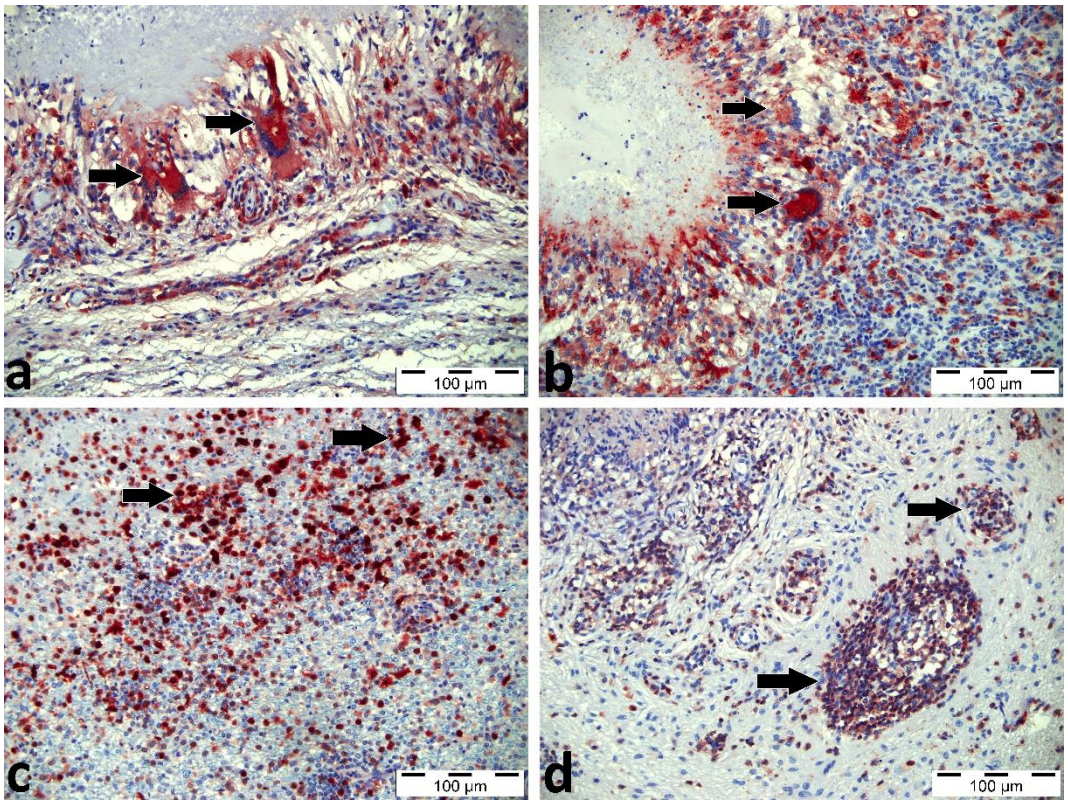


Figure 2. A microscopic view of brain tissues, IHC. a: Strong TNF-α positive expressions in the cytoplasm of foreign body giant cells (arrows), b: Intense intracytoplasmic IFN-γ positive stainings in foreign body giant cells around the cyst wall (arrows), c: Strong IL-1β immunoreactivity in glial cells (arrows), d: IL-2 expression in perivascular inflammatory cell infiltration (arrows).

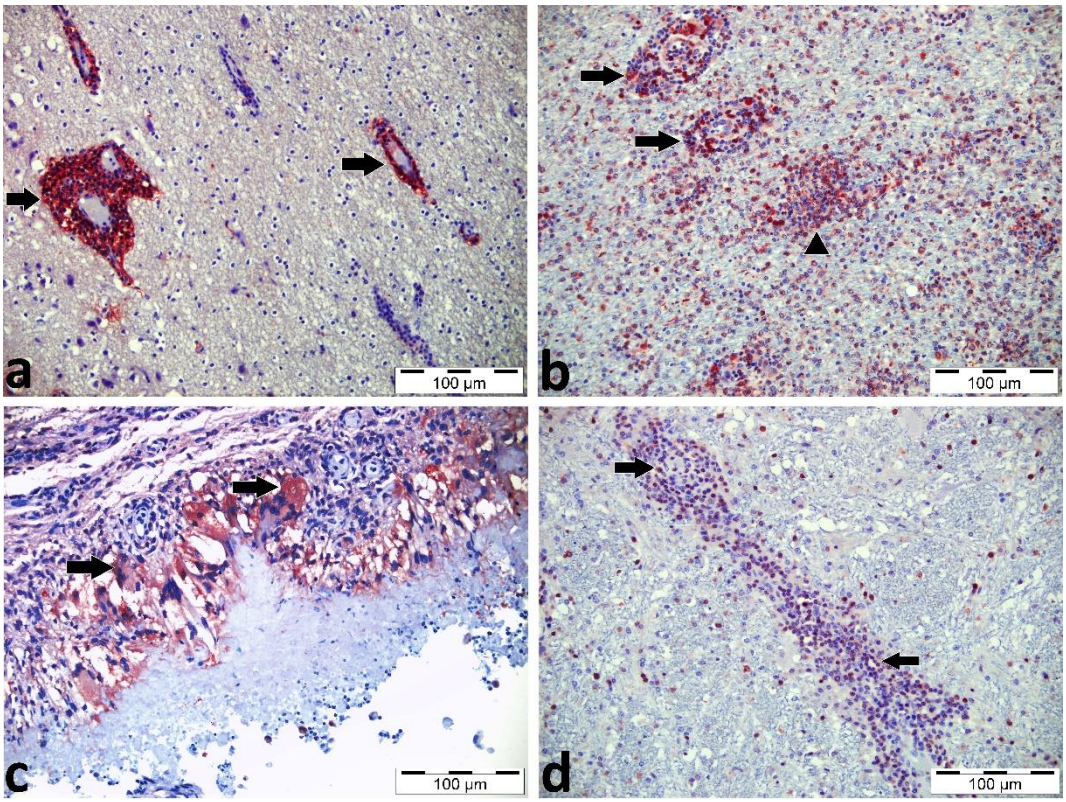


Figure 3. A microscopic view of brain tissues, IHC. a: Strong IL-6 positive stainings in perivascular cuffings (arrows), b: IL-8 expressions in perivascular mononuclear inflammatory cell infiltrations (arrows) and glial cells (arrowhead), c: Intracytoplasmic IL-10 immunoreactivity in foreign body giant cells around the cyst membrane (arrows), d: IL-12 immunopositive stainings around the vessels (arrows).

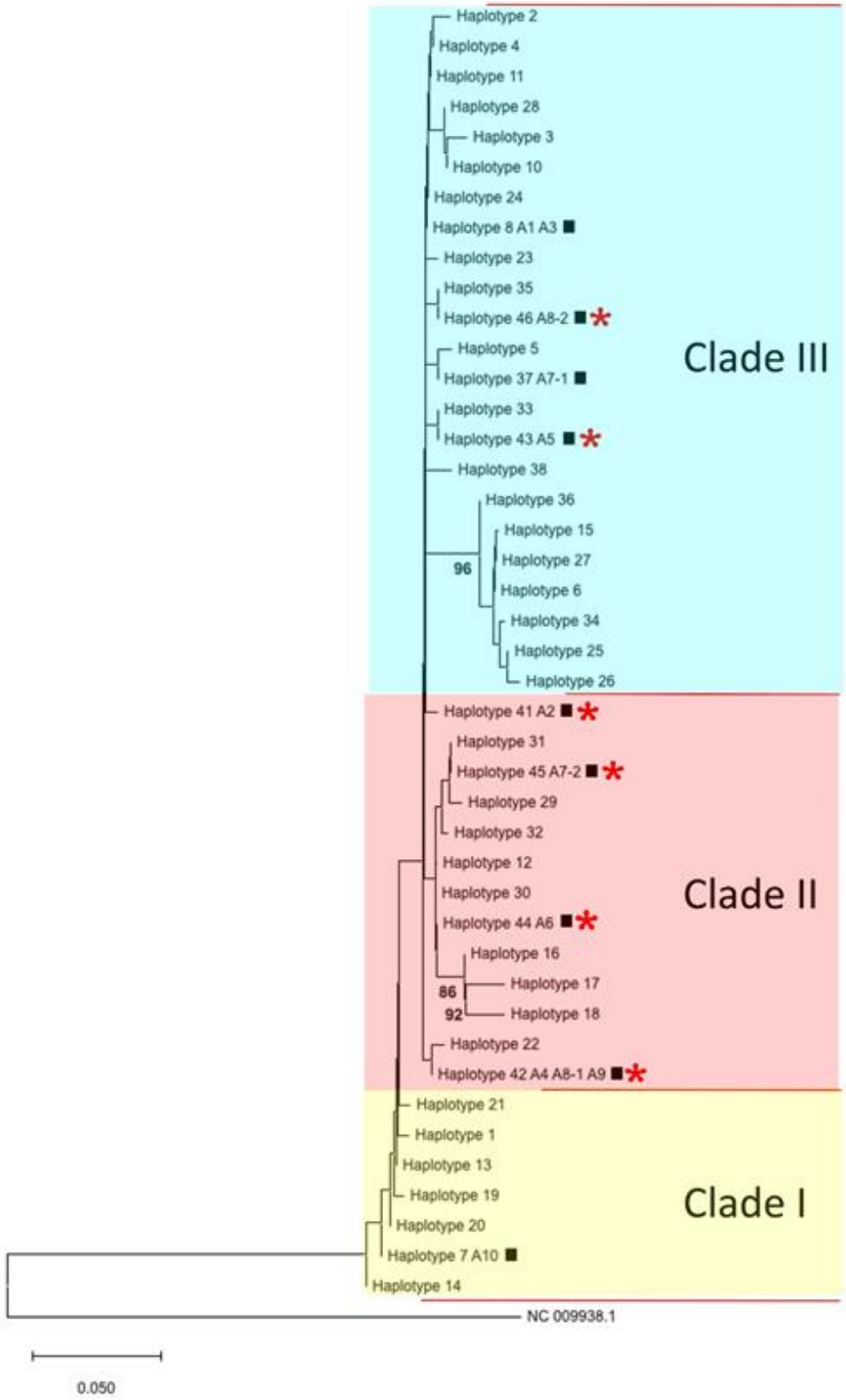


Figure 4. A phylogenetic tree of *Coenurus cerebralis* isolates based on ND1 gene. A NJ tree was constructed using the Kimura 2-parameter model in MEGA12 (34, 35, 50, 53). Bootstrap values derived from 1000 replicates are shown at the nodes; only values ≥70% are indicated (19). The scale bar represents a genetic distance of 0.050 substitutions per site. The NC_009938.1 was used as the outgroup. ■: Haplotypes containing isolates obtained in the present study. ■*: Denotes unique haplotypes exclusively represented by isolates identified in this study.

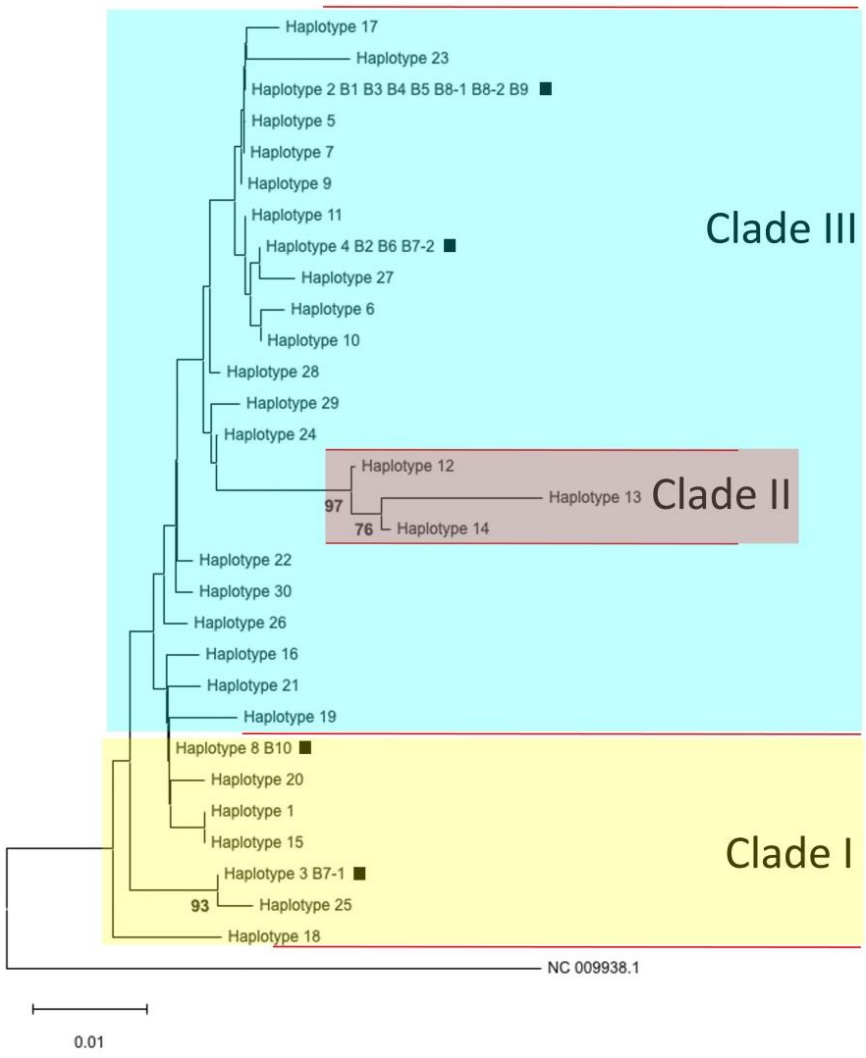


Figure 5. A phylogenetic tree of *Coenurus cerebralis* isolates based on COX1 gene. A NJ tree was constructed using the Kimura 2-parameter model in MEGA12 (34, 35, 50, 53). Bootstrap values derived from 1000 replicates are shown at the nodes; only values ≥70% are indicated (19). The scale bar represents a genetic distance of 0.01 substitutions per site. The NC_009938.1 was used as the outgroup. ■: Haplotypes containing isolates obtained in the present study.

Table 1. Information about sheep and localization of cysts.

Case IDs	Gender	Age	The number of *C. cerebralis*	Localization
1	Female	5 months	2	CH (RFL and LFL)
2	Male	12 months	1	CH (RFL)
3	Female	6 months	1	CH (LPL)
4	Male	9 months	1	CH (LPL)
5	Male	12 months	1	CH (RPL)
6	Female	8 months	2	CH (RPLand LPL)
7	Male	9 months	2	CH (RFLand LFL)
8	Male	12 months	3	CH (RPL and LPL) and C
9	Male	9 months	1	CH (RFL)
10	Female	12 months	1	CH (LFL)

CH: Cerebral hemispheres, C: Cerebellum, RFL: Right frontal lobe, LFL: Left frontal lobe, LPL: Left parietal lobe, RPL: Right parietal lobe.

Table 2. The information of primary antibodies used in immunohistochemical analysis.

Primary antibodies	Clonality	Dilution	Company and Catalog no
TNF-α	Monoclonal	1:100	MyBioSource USA, MBS2025729
IFN-γ	Polyclonal	1:100	MyBioSource USA, MBS2091397
IL-1β	Polyclonal	1:50	MyBioSource USA, MBS2026862
IL-2	Polyclonal	1:200	Biorbyt Ltd. UK, orb657069
IL-6	Monoclonal	1:100	MyBioSource USA, MBS2012740
IL-8	Polyclonal	1:200	MyBioSource USA, MBS2004056
IL-10	Polyclonal	1:200	MyBioSource USA, MBS2026258
IL-12	Polyclonal	1:50	MyBioSource USA, MBS1490500

Table 3. Nucleotide variation sites of the ND1 gene.

| Haplotypes | Accession numbers / Sample IDs | Nucleotide positions* | | |

Table 4. Nucleotide variation sites of the COX1 gene.

Haplotypes	Accession numbers / Sample IDs	Nucleotide positions*																																		
		768	771	793	795	816	822	837	847	853	861	863	867	882	883	891	900	901	909	917	938	1002	1011	1019	1022	1029	1035	1041	1050	1055	1056	1092	1094
Hap-1	NC_012894.1: 6891-8513 (Ref. acces.) / Gene ID 8097137*	C	A	C	A	T	A	A	T	A	G	G	C	A	G	A	G	A	A	G	G	G	T	G	G	T	T	A	T	G	T	A	G
Hap-2	JQ710576.1, OR239757.1, OR239759.1, OR239763.1, OR239764.1, KR604808.1, KT217577.1, KT217590.1, KT217595.1, PQ213612.1, PQ213613.1, PQ213616.1, PQ213620.1, PQ213628.1, PQ213643.1, B1, B3, B4, B5, B8-1, B8-2, B9	T	.	.	G	.	.	.	.	.	.	.	T	.	.	.	.	.	G	.	.	.	C	.	.	.	.	.	.	.	.	.	.
Hap-3	JQ710587.1, KX511892.1, LC271694.1, B7-1	.	.	.	.	.	G	G	.	.	.	.	T	G	.	.	.	.	.	.	.	.	.	.	.	.	.	.	.	.	.	.	.
Hap-4	OR239756.1, OR239760.1, KT253933.1, KT253934.1, JX507239.1, FR873148.1 MZ713179.1, MZ713180.1, PQ213625.1, PQ213631.1, PQ213632.1, B2, B6, B7-2	T	.	.	.	.	.	.	.	.	.	.	T	.	.	.	.	.	G	.	.	.	C	.	.	.	.	.	.	.	.	.	.
Hap-5	OR239758.1	T	.	.	G	.	.	.	.	.	.	.	T	.	.	.	.	.	G	.	.	.	C	.	.	.	.	.	.	.	.	-	-
Hap-6	OR239761.1	-	T	.	.	.	.	.	.	.	.	.	T	.	.	.	.	.	G	.	.	.	C	.	.	.	.	.	.	.	.	.	.
Hap-7	OR239762.1	T	.	.	G	.	.	.	.	.	.	.	T	.	.	.	.	.	G	.	.	.	C	.	.	.	.	.	.	.	.	-	-
Hap-8	EF393620.1, PQ213606.1, KR604810.1, PP907960.1, PP907963.1, PP907962.1, PQ213618.1, PQ213621.1, PQ213627.1, PQ213629.1, PQ213634.1, B10	.	.	.	.	.	.	.	.	.	.	.	T	.	.	.	.	.	.	.	.	.	.	.	.	.	.	.	.	.	.	.	.
Hap-9	PP713059.1	-	-	.	G	.	.	.	.	.	.	.	T	.	.	.	.	.	G	.	.	.	C	.	.	.	.	.	.	.	.	.	.
Hap-10	PP711257.1	-	-	-	-	-	-	.	.	.	.	.	T	.	.	.	.	.	G	.	.	.	C	.	.	.	.	.	.	.	.	.	.
Hap-11	PP711299.1	-	-	-	-	-	-	.	.	.	.	.	T	.	.	.	.	.	G	.	.	.	C	.	.	.	.	.	.	.	.	.	.
Hap-12	HM143882.1	T	.	.	.	.	.	.	.	.	C	C	T	.	.	.	.	.	G	.	.	.	.	C	C	.	.	.	.	.	.	.	.
Hap-13	HM143884.1	T	.	.	.	.	.	.	.	.	C	C	T	.	T	.	.	T	G	.	C	.	C	C	C	.	A	.	.	C	.	.	.
Hap-14	HM143886.1	T	.	.	.	.	.	.	.	.	C	C	T	.	T	.	.	.	G	.	.	.	.	C	C	.	.	.	.	.	.	.	.
Hap-15	KR604811.1, GQ228818.1	.	.	.	.	.	.	.	.	.	.	.	.	.	.	.	.	.	.	.	.	.	.	.	.	.	.	.	.	.	.	.	.
Hap-16	KR604807.1, PQ213626.1, PQ213638.1	.	.	T	.	.	.	.	.	.	.	.	T	.	.	.	.	.	.	.	.	.	.	.	.	.	.	.	.	.	.	.	.
Hap-17	KR604809.1	T	.	.	G	.	.	.	.	.	.	.	T	.	.	G	.	.	G	.	.	.	C	.	.	.	.	.	.	.	.	.	.
Hap-18	MZ346598.1	.	.	.	.	.	.	.	.	.	.	.	T	.	.	.	.	.	.	C	.	T	.	.	.	.	.	G	.	.	.	G	.
Hap-19	FJ886783.1	.	.	.	.	.	.	.	.	.	.	.	T	.	.	.	A	.	.	.	.	.	.	.	.	.	.	.	.	.	.	.	A
Hap-20	DQ309769.1, FJ744755.1	.	.	.	.	.	.	.	.	.	.	.	T	.	.	.	.	.	.	.	.	.	.	.	.	.	.	.	.	.	C	.	.
Hap-21	DQ321830.1	.	.	.	.	C	.	.	.	.	.	.	T	.	.	.	.	.	.	.	.	.	.	.	.	.	.	.	.	.	.	.	.
Hap-22	KX547633.1	T	.	.	G	.	.	.	.	.	.	.	T	.	.	.	.	.	.	.	.	.	.	.	.	.	.	.	.	.	.	.	.
Hap-23	AB792725.1	T	.	.	G	.	.	C	.	.	.	.	T	.	.	.	.	.	G	.	.	.	C	.	.	C	.	.	C	.	.	.	.
Hap-24	OP782685.1, MK189452.1	T	.	.	.	.	.	.	.	.	.	.	T	.	.	.	.	.	G	.	.	.	.	.	.	.	.	.	.	.	.	.	.
Hap-25	LC271741.1	.	.	.	.	.	G	G	.	G	.	.	T	G	.	.	.	.	.	.	.	.	.	.	.	.	.	.	.	.	.	.	.
Hap-26	PQ213607.1	.	.	.	G	.	.	.	.	.	.	.	T	.	.	.	.	.	.	.	.	.	.	.	.	.	.	.	.	.	.	.	.
Hap-27	PQ213614.1	T	.	.	.	.	.	.	C	.	.	.	T	.	.	.	.	.	G	.	.	.	C	.	.	.	.	.	.	.	.	.	.
Hap-28	PQ213630.1	T	.	.	G	.	.	.	.	.	.	.	T	.	.	.	.	.	G	.	.	.	.	.	.	.	.	.	.	.	.	.	.
Hap-29	PQ213636.1	.	.	.	.	.	.	.	.	.	.	.	T	.	.	.	.	.	G	.	.	.	.	.	.	.	.	.	.	.	.	.	.
Hap-30	MT556443.1	T	.	.	.	.	.	.	.	.	.	.	T	.	.	.	.	.	.	.	.	.	.	.	.	.	.	.	.	.	.	.	.

Colors indicate host species. Dark blue: Sheep, Purple: Goat, Light blue: Cattle, Green: Dog, Black: Yak, Red: Study samples.

Table 5. Immunopositivity scores according to granuloma formations, clinical findings and the association between mitochondrial haplotypes.

Case IDs	Granuloma formation	Clinical symptoms	TNF-α	IFN-γ	IL-1β	IL-2	IL-6	IL-8	IL-10	IL-12	ND1 haplotype: Clade	COX1 haplotype: Clade
1	+	+++	+++	+++	++	+++	++	+++	++	+++	A1: Clade III	B1: Clade III
2	-	++	+	++	+	+	+	+	++	++	A2: Clade II	B2: Clade III
3	-	+	++	+++	+	+	+	+++	++	+	A3: Clade III	B3: Clade III
4	-	+	++	++	+	+	+	++	+	++	A4: Clade II	B4: Clade III
5	+	+++	+++	+++	+++	+++	+	++	+	+++	A5: Clade III	B5: Clade III
6	+	+++	+++	+++	++	++	+	+++	++	++	A6: Clade II	B6: Clade III
7	+	++	+++	+++	++	+++	+	++	++	++	A7-1: Clade III A7-2: Clade II	B7-1: Clade I B7-2: Clade III
8	+	+++	+++	+++	++	++	+	+++	+	++	A8-1: Clade II A8-2: Clade III	B8-1: Clade III B8-2: Clade III
9	+	+++	+++	+++	+++	+++	++	+++	+	+++	A9: Clade II	B9: Clade III
10	-	+	+	++	+	+	+	+	+	+	A10: Clade I	B10: Clade I

Discussion and Conclusion

Coenurosis, caused by the *C. cerebralis*, is a significant zoonotic parasitic disease that results in considerable economic difficulties within the livestock industry (60). The present study investigating the haplotypic diversity of *T. multiceps* in Türkiye evaluated potential correlations with the patterns of granuloma formation, clinical symptoms, and cytokine expression.

Determination of cytokine levels has been used in numerous studies to evaluate the immune response to parasitic infections in ruminants (8, 52, 57). The literature reviews revealed a limited number of studies assessing the immune response to *C. cerebralis*.

TNF-α facilitates the activation of phagocytic cells to suppress the replication of intracellular parasites, aiding in the clearance of these pathogens (52). Furthermore, TNF-α plays a critical role in the regulation of inflammation in numerous diseases, such as Neurocysticercosis (NCC), which leads to meningitis and autoimmune encephalitis (39). IFN-γ plays a crucial role in restricting intracellular replication and, particularly during the early stages of infection, activates macrophage-mediated processes to eliminate intracellular pathogens (52). On the other hand, IFN-γ, primarily produced by natural killer (NK) cells during the innate immune response, can activate macrophages, enhancing their phagocytic capacity and cytotoxic abilities (20). In the present study, the expression of TNF-α and IFN-γ expressions were most notably intensified in the cytoplasm of foreing body giant cells. The immunohistochemical findings of this study highlight the critical role of both TNF-α and IFN-γ in macrophage activation.

Granulomas are conventionally linked to an inflammatory Th1 response in the presence of the invasive microorganism or parasite. The Th1 immune response is most prevalent in early-stage granulomas (during the acute phase of infection), whereas a mixed Th1/Th2 immune response occurs mainly in advanced-stage granulomas (during the chronic phase of infection) (22). In NCC, both Th1 (IFN-γ and IL-18) and Th2 (IL-4, IL-18, and IL-10) cytokines are found in brain granulomas surrounding dead parasites. On the other hand, Th1 cytokines (IL-2 and IFN-γ) are found to be highly effective in peritoneal granulomas induced in mice, following infection with *Taenia crassiceps* (20, 33). A strong correlation exists between the Th1 immune response, characterized by the production of cytokines such as TNF-α, IFN-γ and IL-10, and the Th2 immune response in granuloma formation in NCC (47). The current study's data reveals that the immune response to *C. cerebralis*, particularly the granulomatous inflammatory reaction, is largely characterized by Th1-type responses and M1 macrophage activation. In addition, immunohistochemical data shows that although anti-inflammatory cytokines (Th2) like IL-10 and IL-6 also play a role in granuloma formation, pro-inflammatory cytokines such as IFN-γ and TNF-α is more efficient in this process.

Pro-inflammatory cytokine levels like IFN-γ, TNF-α, and IL-1β are more much more dominant in symptomatic NCCs, whereas the levels of IL-10, an anti-inflammatory cytokine, is considerably more dominant in asymptomatic NCCs. The granulomatous response that develops against dying cysts in NCC triggers seizures, and the synthesis of Th1 cytokines including IFN-γ, IL-2 and IL-12 are quite effective in this granulomatous response.

The levels of Th2 cytokines are lower compared to Th1 cytokines (46, 61). Similarly, inflammation is recognized as the primary component associated with the severity of the infection in NCC. It is known that pro-inflammatory cytokines such as IL-6, TNF-α and IFN-γ, which are involved in the neuroinflammatory response to this disease, are closely related to the severity of NCC (20). Some cytokine genes are crucial for resistance to parasites. IL-1β, a key pro-inflammatory cytokine, supports the initiation of the early immune response (9). In contrast to human NCC, an inflammatory immune response characterized by increased production of IL-1β, TNF-α, and IFN-γ is triggered (47). This study confirmed the literature data, revealing that clinical findings were much more severe in cases with granuloma formation and progressed in a wide range. In these cases where clinical findings are more severe, Th1 type cytokines such as TNF-α, IFN-γ, IL-1β, IL-2, IL-8, and IL-12 demonstrated more efficacy, while in cases with mild or unremarkable clinical signs, Th2 type cytokines IL-10 and IL-6 were found to be more effective.

IL-2 induces an effective cellular defence that is essential for eliminating intracellular parasites in the early stages of infection (54). Decreased IL-2 levels may inhibit the proliferation of T and B cells, hence promoting the localization and survival of the parasite (20). The IL-1β positive staining was mostly concentrated in the lymphocytes located around the vessels close to the areas where the parasitic organism was located in our study. In parallel with IL-1β immunoreactivity, IL-2 positive staining was much more prevalent in cases of granuloma formation. The localization of IL-1β and IL-2 immunopositive staining in the current study confirmed the antiparasitic effects of these cytokines in granuloma formation against *C. cerebralis*. A correlation was observed between the severity of clinical findings and IL-1β and IL-2 expression.

IL-6 and IL-8 are produced by a variety of cell types, the most important sources of these cytokines being macrophages and monocytes in inflammatory areas. IL-6, a monocyte-derived effector cytokine, plays a critical role in the development of cellular and humoral defense. It helps the recruitment of monocytes to the inflammatory site, can activate endothelial cells to secrete IL-8, monocyte chemotactic protein-1, and initiate the expression of adhesion molecules (51). In the current study, IL-6 expression was present in both granuloma-forming and non-granuloma-forming cases. It was noted that glial cells, histiocytes, and monocytes in inflammatory areas mostly showed IL-6 immunoreactivity. These results show that both cellular and humoral defenses are effective in the immune response against *C. cerebralis*. Besides pro-inflammatory cytokines, IL-6 positive staining demonstrates, that anti-inflammatory cytokines also contribute to immunity against this parasite. IL-8 expression in the CNS causes an influx of monocytes, lymphocytes, and leukocytes (especially neutrophils), associated with increased intracranial pressure, cerebral infarction, and encephalitis (30, 51). In this study, IL-8 positive reactions were primarily in macrophage-derived cells. IL-8 immunopositivity was significantly elevated in instances characterized by prominent clinical symptoms, granuloma formation, and severe inflammatory responses matching the patterns observed with other Th1 cytokines.

The interleukin-10 produced by M2 macrophages exhibits anti-inflammatory properties (43). IL-10 inhibits the release of proinflammatory cytokines from microglial and resident glial cells, therefore exhibiting an anti-inflammatory effect (40). It was noted that glial cells as well as foreign body giant cells reacted positively in terms of IL-10 expression in the current study. Additionally, IL-10 is also linked to humoral immunity (54). IL-10 is essentially a Th2 cytokine and significantly contributes to the suppression of the host's immune response. A study revealed that IL-10 levels were significantly increased in patients with NCC compared to healthy individuals in the control group (21). Likewise, it has been reported that IL-10 is released in both clinically symptomatic and asymptomatic cases (46). In the current study, it was observed that IL-10 was expressed in both granuloma-formed and non-granuloma-formed caseswith mild and/or severe clinical findings. Under the scope of these, IL-10 appears to play a regulatory role in the immune response to *C. cerebralis*.

It has been widely accepted that IL-12, which is produced by B lymphocytes and macrophages, has the ability to induce Th1-associated response by stimulating IFN-γ production from T cells and NK cells. The stimulation of IFN-γ production by IL-12 has been demonstrated to increase protective immunity against some intracellular parasites, such as *Leishmania major*. This cytokine plays an important role for the endogenous regulation of the granulomatous response in *Schistosoma mansoni* infection (32). The present study showed that IL-12 positive reactions correlated with other Th1 cytokines regarding granuloma formation and clinical findings. The immunostaining intensities of IL-12 and IFN-γ were observed to be remarkably correlated.

Despite the increasing number of molecular studies on *T. multiceps*, current knowledge of its global haplotype diversity remains fragmented and remain limited, with available data originating from Italy (58, 59), Egypt (6), Pakistan (5), and a study which was conducted from Greece, United Arab Emirates, India, Iran, Sudan, Oman, Somalia, Yemen, Bangladesh, Ethiopia (16) and additionally, recent analyses have utilized previously deposited *T. multiceps* sequences from multiple countries through GenBank-based comparative studies (1, 24, 26).

Similarly, studies conducted on haplotype variability of *T. multiceps* in Türkiye are also limited. Çelik et al. (15) analyzed 39 sheep isolates using both COX1 and ND1 gene regions and reported a multiple coenurosis case demonstrating COX1 haplotype diversity (14). To contribute to the limited existing data, haplotype analyses of both the COX1 and ND1 gene regions were performed in the present study.

The ND1-based NJ topology indicates that the analyzed haplotypes are structured into three shallow but distinct clades rather than into deeply divergent lineages. This pattern suggests limited historical divergence within the group, with several well-supported sub-clades reflecting recent diversification of closely related ND1 haplotypes. Although the haplotypes originated from different countries and even different continents, they were intermingled within Clades I–III, and no clear continental or country-specific clustering was observed (Figure 4, Table 3). This observation aligns with previous ND1-based studies, which likewise demonstrated no region-specific or host-specific phylogenetic structuring among *T. multiceps* isolates (1, 6, 16, 60). Thus, the ND1 phylogeny did not reveal any obvious phylogeographic structuring, which may reflect extensive historical gene flow among populations and/or the retention of shared ancestral polymorphism across the regions of included all sequence data. The COX1-based NJ topology further supported the presence of three shallow, closely related clades rather than deeply divergent lineages. Clade I contained the most basal lineages, including some of the previously described reference sequences (B7-1 and B10), whereas Clade II represented a small but well-supported subclade of closely related haplotypes that branched from Clade III. Clade III encompassed the largest set of COX1 haplotypes and included most of the published COX1 lineages (B1-B9), which were interspersed with the newly identified haplotypes instead of forming distinct monophyletic units. As in the ND1 tree, haplotypes derived from different countries and continents were scattered across Clades I–III, and no clear continent- or country-specific clustering was observed (Figure 5, Table 4). Similarly, the COX1 phylogeny did not reveal any obvious phylogeographic structuring, which is consistent with extensive historical gene flow and/or the persistence of shared ancestral polymorphism across the analyzed populations. Similarly, previous COX1-based studies have reported an absence of region- or host-associated phylogenetic segregation among *T. multiceps* isolates (6, 24, 60). Overall, the concordant ND1- and COX1-based topologies indicate that, despite the broad geographic origin of the samples, mitochondrial variation is shallow and largely shared among populations, pointing to a single, widely distributed gene pool rather than regionally differentiated lineages.

Several studies have documented the presence of multiple *C. cerebralis* in the brain (3, 7, 14, 31, 59). In the present study, four sheep were observed with multiple *Coenurus* cysts (Table 1). However, only two sheep with two cysts, could be molecularly analyzed with both ND1 and COX1 genes; the remaining animals with multiple cysts could not be studied representing a limitation of our study. The cysts from both animals displayed distinct haplotypes based on the ND1 gene sequence, while one animal's cysts demonstrated separate haplotypes based on the COX1 gene sequence. This indicates that the animals were exposed to *T. multiceps* eggs at varying intervals or that *T. multiceps* eggs with distinct genetic characteristics coexisted simultaneously in the same pasture. This could relate to the environmental factors influencing the viability of *T. multiceps* eggs; for example, the eggs have been recorded to survive for one year (28). Although multiple cysts were molecularly examined in two animals, the number of samples was insufficient to evaluate statistically a possible correlation between multiple *Coenurus* infections and haplotype specificity. Varcasia et al. (59) also found no statistical correlation despite analyzing a considerably larger number of multicystic cases (13 out of 47), which is consistent with the findings of the present study. Further research is needed to determine the specific environmental factors that influence the occurrence of the unique haplotypes. This procedure should be conducted for each cyst found in an intermediate host to better understand genetic variations in *T. multiceps*.

In the present study, although several nucleotide polymorphisms were detected across the four sequences (Sample IDs 7 and 8), all changes within the analyzed COX1 fragment were synonymous; no amino acid-altering substitutions were observed. This pattern is consistent with the well-documented functional constraint and relative amino-acid conservation of mitochondrial COX1-one reason it is widely used for DNA barcoding and phylogenetic inference in animals and helminths (4, 27, 37, 41).

Taken together, the limited number of cases analysed did not allow any statistical inference regarding the relationship between mitochondrial haplotypes and neuropathological/immunohistochemical patterns. Overall, the pathological and cytokine profiles appeared to be broadly comparable across the different ND1-COX1 haplotypes and clades, suggesting that, within the our present results, host immune responses are driven more by general parasite burden and lesion stage than by specific mitochondrial lineages.

In conclusion, despite the limited sample size in the present study, data from eight different pro-inflammatory and anti-inflammatory cytokines were assessed, revealing comprehensive cytokine profiles in the immune response to *C. cerebralis*. The immune response to *C. cerebralis* exhibits a mixed Th1/Th2 profile, predominantly

characterized by Th1 cytokines. TNF-α and IFN-γ were strongly associated with macrophage activation and granuloma formation, indicating their importance in cellular immune response. IL-6 and IL-10 positivity suggests that humoral and anti-inflammatory pathways also contribute to the response. In this study, high genetic diversity was identified for both ND1 and COX1. These are widely used mitochondrial markers for lineage/genotype discrimination and molecular diagnosis in *T. multiceps*. The literature documents substantial haplotype diversity across geographies and hosts and, in some datasets, epidemiological associations with tissue tropism or clinical presentation (cerebral vs. extra-cerebral coenurosis). However, there is no direct evidence that phenotypic differences are causally driven by specific substitutions in COX1/ND1; these loci function primarily as lineage markers. It is suggested that *C. cerebralis* remains an ongoing problem, requiring the investigation of each distinct genetic variation for disease prevention and control.

Financial Support

This research received no grant from any funding agency/sector.

Ethical Statement

This study was approved by the Kafkas University Animal Experiments Local Ethics Committee (KAU-HADYEK/2022-008).

Conflict of Interest

The authors declare that they have no conflict of interest. Although Gökben ÖZBAKIŞ BECERİKLİSOY is a member of the Editorial Board of the journal, she was not involved in the peer-review process or in the editorial decision concerning this manuscript.

Author Contributions

EK and GÖB conceived the idea and planned the manuscript. EK, GÖB and BÇ contributed to methodology. All authors contributed to investigation; GÖB and BÇ contributed to molecular analyses and data curation. HN and AYU performed systemic necropsy and histopathological and immunohistochemical staining. EK, EB and SD performed histopathological and immunohistochemical analyses. GÖB, EK, and BÇ wrote the original draft preparation. All authors provided significant contributions by giving feedback and help shape the manuscript.

Data Availability Statement

The data supporting this study's findings are available from the corresponding author upon reasonable request. The resulting nucleotide sequences were submitted to the GenBank database with the following accession numbers PX671641-PX671652 for COX1 and PX677447-PX677458 for ND1.

Declaration of Generative Artificial Intelligence

The authors declare that generative artificial intelligence (AI) and AI-assisted technologies were not used in the writing of this manuscript. AI-assisted tools were used solely for language editing purposes to improve grammar and readability.

Animal Welfare

The authors confirm that they have adhered to ARRIVE Guidelines to protect animals used for scientific purposes.

References

1. **Abbas I, El-Alfy ES, Saleh S, et al** (2022): *Global epidemiology and molecular biology of Taenia multiceps: a comparative meta-analysis and in silico analysis study.* Parasitology, **149**, 1607-1622. DOI: 10.1017/S0031182022001123.
2. **Abbas I, Tamponi C, Madau G, et al** (2024): *Treatment and management of coenurosis by Taenia multiceps: field data from outbreaks in endemic regions and literature review*. Parasit Vectors, **17**, 335. DOI: 10.1186/s13071-024-06430-2.
3. **Akkuş E, Oğuz FE** (2024): *Molecular prevalence of Coenurus cerebralis in sheep with neurological symptoms in Iğdır Province, Türkiye*. Pak Vet J, **44**, 499-503. DOI: 10.29261/pakvetj/2024.186.
4. **Al Malki JS, Hussien NA** (2021): *Molecular characterization and phylogenetic studies of Echinococcus granulosus and Taenia multiceps coenurus cysts in slaughtered sheep in Saudi Arabia.* Open Life Sci, **16**, 1252-1260. DOI: 10.1515/biol-2021-0131.
5. **Alvi MA, Ohiolei JA, Saqib M, et al** (2020): *First report on molecular characterization of Taenia multiceps isolates from sheep and goats in Faisalabad, Pakistan.* Front Vet Sci, **7**, 594599. DOI: 10.3389/fvets.2020.594599.
6. **Amer S, ElKhatam A, Fukuda Y, et al** (2017): *Prevalence and identity of Taenia multiceps cysts "Coenurus cerebralis" in sheep in Egypt.* Acta Trop, **176**, 270-276. DOI: 10.1016/j.actatropica.2017.08.012.
7. **Anwar S, Mahdy E, El-Nesr KA, et al** (2013): *Monitoring of parasitic cysts in the brains of a flock of sheep in Egypt.* Rev Bras Parasitol Vet, **22**, 323-330. DOI: 10.1590/s1984-29612013000300002.
8. **Attia MM, El-Gameel SM, Ismael E** (2020): *Evaluation of tumor necrosis factor-alpha (TNF-α); gamma interferon (IFN-γ) genes and oxidative stress in sheep: immunological responses induced by Oestrus ovis (Diptera: Oestridae) infestation.* J Parasit Dis, **44**, 332-337. DOI: 10.1007/s12639-020-01220-w.
9. **Attia MM, Soliman SM, Mahmoud MA, et al** (2022): *Oxidative stress markers, immune-regulating cytokines, and the pathological evaluation of sheep co-infected with Oestrus ovis and Coenurus cerebralis.* Microb Pathog, **169**, 105613. DOI: 10.1016/j.micpath.2022.105613.

10. **Avcioglu H, Yildirim A, Duzlu O, et al** (2011): *Prevalence and molecular characterization of bovine coenurosis from Eastern Anatolian region of Turkey.* Vet Parasitol, **176**, 59-64. DOI: 10.1016/j.vetpar.2010.10.033.
11. **Biçek K, Karakuş A, Değer MS** (2019): *Van ilinde Coenurus cerebralis'in yaygınlığı ve coenurosis'in teşhisinde yardımcı bir parametre olarak enolaz (NSE) enziminin önemi*. Atatürk Univ Vet Bilim Derg, **14**, 185-192. DOI: 10.17094/ataunivbd.518785.
12. **Bowles J, Blair D, McManus DP** (1992): *Genetic variants within the genus Echinococcus identified by mitochondrial DNA sequencing.* Mol Biochem Parasitol, **54**, 165-173. DOI: 10.1016/0166-6851(92)90109-w.
13. **Bowles J, McManus DP** (1993): *NADH dehydrogenase 1 gene sequences compared for species and strains of the genus Echinococcus.* Int J Parasitol, **23**, 969-972. DOI: 10.1016/0020-7519(93)90065-7.
14. **Celik F, Tekin AS, Uslug M, et al** (2025): *Multiple Coenurus cerebralis cysts detected in a sheep brain and molecular characterization of the individual cysts.* Vet Ital, **61**. DOI: 10.12834/VetIt.3437.24057.2.
15. **Celik F, Uslug M, Tekin AS, et al** (2025): *High genetic variability in Taenia multiceps larvae: a mitochondrial DNA-based study of sheep isolates using CO1 and NADH1 genes*. Res Vet Sci, **195**, 105863. DOI: 10.1016/j.rvsc.2025.105863.
16. **Christodoulopoulos G, Dinkel A, Romig T, et al** (2016): *Cerebral and non-cerebral coenurosis: on the genotypic and phenotypic diversity of Taenia multiceps*. Parasitol Res, **115**, 4543-4558. DOI: 10.1007/s00436-016-5246-4.
17. **Çiftçi DA, Yücesan B** (2025): *Identification and prevalence of Coenurus cerebralis in sheep: Diyarbakır example*. Turk Hij Den Biyol Derg, **82**, 131-138. DOI: 10.5505/TurkHijyen.2025.53077.
18. **Deplazes P, Eichenberger RM, Grimm F** (2019): *Wildlife-transmitted Taenia and Versteria cysticercosis and coenurosis in humans and other primates.* Int J Parasitol Parasites Wildl, **9**, 342-358. DOI: 10.1016/j.ijppaw.2019.03.013.
19. **Felsenstein J** (1985): *Confidence limits on phylogenies: an approach using the bootstrap*. Evolution, **39**, 783-791. DOI: 10.2307/2408678.
20. **Fleury A, Alaez C, Dessein A, et al** (2018): *No association of IL2, IL4, IL6, TNF, and IFNG gene polymorphisms was found with Taenia solium human infection or neurocysticercosis severity in a family-based study.* Hum Immunol, **79**, 578-582. DOI: 10.1016/j.humimm.2018.04.011.
21. **Fleury A, Cardenas G, Adalid-Peralta L, et al** (2016): *Immunopathology in Taenia solium neurocysticercosis.* Parasite Immunol, **38**, 147-157. DOI: 10.1111/pim.12299.
22. **Freitas AA, Moura VBL, Irusta VRC, et al** (2016): *IFN-gamma role in granuloma formation in experimental subcutaneous cysticercosis.* Exp Parasitol, **168**, 1-8. DOI: 10.1016/j.exppara.2016.06.004.
23. **Gasser RB, Zhu X, McManus DP** (1999): *NADH dehydrogenase subunit 1 and cytochrome c oxidase subunit I sequences compared for members of the genus Taenia (Cestoda).* Int J Parasitol, **29**, 1965-1970. DOI: 10.1016/s0020-7519(99)00153-8.
24. **Gunyakti Kilinc S, Celik F, Kesik HK, et al** (2020): *In silico analysis of the biodiversity and conservation status of mitochondrial cytochrome c oxidase subunit 1 (CO1) gene of Taenia multiceps.* Acta Parasitol, **65**, 852-858. DOI: 10.1007/s11686-020-00236-9.
25. **Hall TA** (1999): *BioEdit: a user-friendly biological sequence alignment editor and analysis program for windows 95/98/NT*. Nucleic Acids Symp Ser, **41**, 95-98.
26. **Haq SU, Malik MA, Alshammari A, et al** (2024): *Genetic variation and population structure of Taenia multiceps (Coenurus cerebralis) based on mitochondrial cox1 gene: a comprehensive global analysis.* Infect Genet Evol, **125**, 105676. DOI: 10.1016/j.meegid.2024.105676.
27. **Hebert PDN, Cywinska A, Ball SL, et al** (2003): *Biological identifications through DNA barcodes.* Proc R Soc Lond B, **270**, 313-321. DOI: 10.1098/rspb.2002.2218.
28. **Jansen F, Dorny P, Gabriël S, et al** (2021): *The survival and dispersal of Taenia eggs in the environment: what are the implications for transmission? a systematic review.* Parasit Vectors, **14**, 88. DOI: 10.1186/s13071-021-04589-6.
29. **Kara M, Celik BA, Celik OY, et al** (2025): *Determination of the prevalence and parasite burden of Coenurus cerebralis and Oestrus ovis in sheep in Siirt Province of Türkiye*. Acta Vet Brno, **94**, 13-21. DOI: 10.2754/avb202594010013.
30. **Karakurt E, Coskun N, Beytut E, et al** (2023): *Cytokine profile in lambs naturally infected with sheeppox virus.* Trop Anim Health Prod, **55**, 401. DOI: 10.1007/s11250-023-03823-w.
31. **Karakurt E, Nuhoğlu H, Sarı B, et al** (2019): *Clinical, pathological and parasitological evaluation of Coenurus cerebralis infecting domestic and wild ruminants*. Dicle Univ Vet Fak Derg, **12**, 122-127. DOI: https://izlik.org/JA28ZY38HS.
32. **Khalifa RM, Taele J, Mohamadin HS** (2012): *Studies on some metacestodes immunohistochemical response in mice as a model for human cysticercosis: I. Role of Th1 and Th2 cytokines in experimental liver granuloma of Mesocestoides corti infected mice.* J Egypt Soc Parasitol, **42**, 103-120.
33. **Khumbatta M, Firozgary B, Tweardy DJ, et al** (2014): *Somatostatin negatively regulates parasite burden and granulomatous responses in cysticercosis.* BioMed Res Int, **2014**, 247182. DOI: 10.1155/2014/247182.
34. **Kimura M** (1980): A *simple method for estimating evolutionary rate of base substitutions through comparative studies of nucleotide sequences.* J Mol Evol, **16**, 111-120. DOI: 10.1007/bf01731581.
35. **Kumar S, Stecher G, Suleski M, et al** (2024): *MEGA 12: Molecular evolutionary genetics analysis version 12 for adaptive and green computing.* Mol Biol Evol, **41**, 1-9. DOI: 10.1093/molbev/msae263.
36. **Lema YL, Prodjinotho UF, Makasi C, et al** (2024): *Evaluating the modulation of peripheral immune profile in people living with HIV and (neuro)cysticercosis.* PLoS Negl Trop Dis, **18**, e0012345. DOI: 10.1371/journal.pntd.0012345.
37. **Liu GH, Lin RQ, Li MW, et al** (2011): *The complete mitochondrial genomes of three cestode species of Taenia infecting animals and humans.* Mol Biol Rep, **38**, 2249-2256. DOI: 10.1007/s11033-010-0355-0.

38. **López-Griego L, Nava-Castro KE, López-Salazar V, et al** (2015): *Gender-associated differential expression of cytokines in specific areas of the brain during helminth infection.* J Interferon Cytokine Res, **35**, 116-125. DOI: 10.1089/jir.2013.0141.
39. **Mahanty S, Orrego MA, Cangalaya C, et al** (2017): *TNF-α blockade suppresses pericystic inflammation following anthelmintic treatment in porcine neurocysticercosis.* PLoS Negl Trop Dis, **11**, e0006059. DOI: 10.1371/journal.pntd.0006059.
40. **Moura VBL, Lima SB, Matos-Silva H, et al** (2016): *Cellular immune response in intraventricular experimental neurocysticercosis.* Parasitology, **143**, 334-342. DOI: 10.1017/s0031182015001572.
41. **Nakao M, Sako Y, Yokoyama N, et al** (2000): *Mitochondrial genetic code in cestodes.* Mol Biochem Parasitol, **111**, 415-424. DOI: 10.1016/s0166-6851(00)00334-0.
42. **Olar LE, Tomoiagă VD, Mârza SM, et al** (2024): *Computed tomography and fluorescence spectroscopy blood plasma analysis study for kynurenic acid as a diagnostic approach to chronic coenurosis in sheep*. Life (Basel), **14**, 1121. DOI: 10.3390/life14091121.
43. **Olguín JE, Corano-Arredondo E, Hernández-Gómez V, et al** (2024): *A myeloid-specific lack of IL-4Rα prevents the development of alternatively activated macrophages and enhances immunity to experimental cysticercosis.* Pathogens, **13**, 169. DOI: 10.3390/pathogens13020169.
44. **Otranto D, Wall R** (2024): Veterinary Parasitology, Wiley-Blackwell, Hoboken NJ, USA.
45. **Philipo V, Lupindu AM, Nzalawahe JS** (2024): *Epidemiology and molecular identification of Coenurus cerebralis in sheep and goats in Mpwapwa District, Tanzania: factors to consider in control plans*. Vet Med Int, **2024**, 5055115. DOI: 10.1155/vmi/5055115.
46. **Prasad A, Prasad KN, Gupta RK, et al** (2009): *Increased expression of ICAM-1 among symptomatic neurocysticercosis.* J Neuroimmunol, **206**, 118-120. DOI: 10.1016/j.jneuroim.2008.09.015.
47. **Prodjinotho UF, Lema J, Lacorcia M, et al** (2020): *Host immune responses during Taenia solium neurocysticercosis infection and treatment.* PLoS Negl Trop Dis, **14**, e0008005. DOI: 10.1371/journal.pntd.0008005.
48. **Rodríguez-Sosa M, Rivera-Montoya I, Espinoza A, et al** (2006): *Acute cysticercosis favours rapid and more severe lesions caused by Leishmania major and Leishmania mexicana infection, a role for alternatively activated macrophages.* Cell Immunol, **242**, 61-71. DOI: 10.1016/j.cellimm.2006.09.006.
49. **Rozas J, Ferrer-Mata A, Sánchez-DelBarrio JC, et al** (2017): *DnaSP 6: DNA sequence polymorphism analysis of large data sets. Mol Biol Evol*, **34**, 3299-3302. DOI: 10.1093/molbev/msx248.
50. **Saitou N, Nei M** (1987): *The neighbor-joining method: a new method for reconstructing phylogenetic trees.* Mol Biol Evol, **4**, 406-425. DOI: 10.1093/oxfordjournals.molbev.a040454.
51. **Singh AK, Singh SK, Singh A, et al** (2015): *Immune response to Taenia solium cysticerci after anti-parasitic therapy.* Int J Parasitol, **45**, 749-759. DOI: 10.1016/j.ijpara.2015.05.007.
52. **Soliman SM, Aljahdali NH, Majrashi KA, et al** (2022): *Immune cell reaction associated with Coenurus cerebralis infection in sheep with particular reference to ELISA as a diagnostic tool.* Life (Basel), **12**, 1515. DOI: 10.3390/life12101515.
53. **Stecher G, Tamura K, Kumar S** (2020): *Molecular evolutionary genetics analysis (MEGA) for macOS.* Mol Biol Evol, **37**, 1237-1239. DOI: 10.1093/molbev/msz312.
54. **Terrazas LI** (2008): *The complex role of pro-and anti-inflammatory cytokines in cysticercosis: immunological lessons from experimental and natural hosts.* Curr Top Med Chem, **8**, 383-392. DOI: 10.2174/156802608783790848.
55. **Terrazas LI, Cruz M, Rodriguez-Sosa M, et al** (1999): *Th1-type cytokines improve resistance to murine cysticercosis caused by Taenia crassiceps*. Parasitol Res, **85**, 135-141. DOI: 10.1007/s004360050522.
56. **Tüfekçi E, Akar Y, Ekinci G, et al** (2022): *A case of Coenurus cerebralis in a pregnant Anatolian wild goat (Capra aegagrus aegagrus).* Erciyes Univ Vet Fak Derg, **19**, 55-59. DOI: 10.32707/ercivet.1085266.
57. **Uztimür M, Dörtbudak MB** (2023): *Evaluation of brain injury in goats naturally infected with Coenurus cerebralis; brain specific biomarkers, acute inflammation, and DNA oxidation.* Res Vet Sci, **165**, 105043. DOI: 10.1016/j.rvsc.2023.105043.
58. **Varcasia A, Lightowlers MW, Cattoli G, et al** (2006): *Genetic variation within Taenia multiceps in Sardinia, Western Mediterranean (Italy).* Parasitol Res, **99**, 622-626. DOI: 10.1007/s00436-006-0179-y.
59. **Varcasia A, Pipia AP, Dessì G, et al** (2016): *Morphology and genetic variability within Taenia multiceps in ruminants from Italy*. Vet Parasitol, **223**,181-185. DOI: 10.1016/j.vetpar.2016.04.039.
60. **Varcasia A, Tamponi C, Ahmed F, et al** (2022): *Taenia multiceps coenurosis: a review*. Parasit Vectors, **15**, 84. DOI: 10.1186/s13071-022-05210-0.
61. **Verma A, Prasad KN, Cheekatla SS, et al** (2011): *Immune response in symptomatic and asymptomatic neurocysticercosis.* Med Microbiol Immunol, **200**, 255-261. DOI: 10.1007/s00430-011-0198-x.
62. **Waterhouse AM, Procter JB, Martin DMA, et al** (2009): *Jalview Version 2: a multiple sequence alignment editor and analysis workbench*. Bioinformatics, **25**, 1189-1191. DOI: 10.1093/bioinformatics/btp033.

Publisher's Note

All claims expressed in this article are solely those of the authors and do not necessarily represent those of their affiliated organizations, or those of the publisher, the editors and the reviewers. Any product that may be evaluated in this article, or claim that may be made by its manufacturer, is not guaranteed or endorsed by the publisher.

This article is licensed under a Creative Commons Attribution-NonCommercial 4.0 International License (CC BY-NC 4.0)